Journal of Thermal Analysis and Calorimetry, Vol. 81 (2005) 617–625

HEAT CAPACITIES AND ABSOLUTE ENTROPIES OF UTi_2O_6 AND $CeTi_2O_6$

Marcus H. Donaldson[1], *Rebecca Stevens*[1], *Brian E. Lang*[1], *Juliana Boerio-Goates*[1], *Brian F. Woodfield*[1*], *Robert L. Putnam*[2] *and Alexandra Navrotsky*[2]

[1]Department of Chemistry and Biochemistry, Brigham Young University, Provo, UT 84606, USA
[2]Thermochemistry Facility, Department of Chemical Engineering and Materials Science, University of California, Davis, Davis, CA 95616, USA

As part of a larger study of the physical properties of potential ceramic hosts for nuclear wastes, we report the molar heat capacity of brannerite (UTi_2O_6) and its cerium analog ($CeTi_2O_6$) from 10 to 400 K using an adiabatic calorimeter. At 298.15 K the standard molar heat capacities are (179.46±0.18) J K^{-1} mol^{-1} for UTi_2O_6 and (172.78±0.17) J K^{-1} mol^{-1} for $CeTi_2O_6$. Entropies were calculated from smooth fits of the experimental data and were found to be (175.56±0.35) J K^{-1} mol^{-1} and (171.63±0.34) J K^{-1} mol^{-1} for UTi_2O_6 and $CeTi_2O_6$, respectively. Using these entropies and enthalpy of formation data reported in the literature, Gibb's free energies of formation from the elements and constituent oxides were calculated. Standard free energies of formation from the elements are (–2814.7±5.6) kJ mol^{-1} for UTi_2O_6 and (–2786.3±5.6) kJ mol^{-1} for $CeTi_2O_6$. The free energy of formation from the oxides at T=298.15 K are (–5.31±0.01) kJ mol^{-1} and (15.88±0.03) kJ mol^{-1} for UTi_2O_6 and $CeTi_2O_6$, respectively.

Keywords: *brannerite, $CeTi_2O_6$, enthalpy, entropy, heat capacity, thermodynamic functions, thermodynamics, UTi_2O_6*

Introduction

With post-Cold War dismantlement of nuclear armories and the proliferation of nuclear reactors as an energy source, the storage of commercial- and weapons-grade nuclear waste becomes an important issue. Not only are safety issues related to the actual storage of these materials important, security measures preventing the possible construction of covert nuclear weapons play a major role in deciding the proper treatment of these materials [1, 2].

As part of an ongoing study of the feasibility of using titanate-based compounds as ceramic host matrices for nuclear waste, we report the molar heat capacities and thermodynamic functions of brannerite, UTi_2O_6, and cerium brannerite, $CeTi_2O_6$. Host matrices are intended to allow crystalline incorporation of the radioactive materials making them chemically difficult to extract. Hosts should also provide a solid waste form resistant to corrosion in aqueous environments [3, 4]. Understanding the thermodynamic properties of both of these materials gives valuable information for proper development, accurate performance modeling, and optimization of possible nuclear waste hosts. Brannerite was chosen for study because it exists naturally as a host for uranium metal and is thought to be very stable in open environments and could possibly be doped with other radioactive elements. Cerium has been used as an analog or model for uranium and plutonium containing compounds because of its high molecular mass and similarity to actinide metals.

Crystallographically, brannerite is monoclinic with space group $C2/m$ with cell parameters a=9.8123(15), b=3.7697(6), c=6.9253(9) Å, β=118.957(6)°, and the coordination of the oxygens around the uranium atoms is a distorted octahedron [5]. Cerium brannerite ($CeTi_2O_6$) is also monoclinic with the following parameters: a=9.84, b=3.75, c=6.91 Å, β=119.15° [6]. The similar sizes of the unit cells further suggests that cerium and uranium compounds should exhibit similar chemical behavior.

Currently, little thermodynamic data and no heat capacity measurements exist for these compounds. As part of this project, the enthalpies of formation of both UTi_2O_6 and $CeTi_2O_6$ were measured earlier by Putnam *et al.* [7]. In this paper we present the results obtained from heat capacity measurements using an adiabatic calorimeter over the temperature range 10–400 K.

Experimental

Sample preparation and characterization

Cerium brannerite was prepared by ball-milling 99.9% pure CeO_2 and TiO_2 (anatase). This mixture was pressed into a pellet and sintered in air at 1623 K for more than 100 h. Uranium brannerite was prepared in a similar

* Author for correspondence: brian_woodfield@chem.byu.edu

1388–6150/$20.00

Akadémiai Kiadó, Budapest, Hungary
Springer, Dordrecht, The Netherlands

manner by heating a powdered mixture of high purity UO_2 and 99.9% pure TiO_2 (anatase) for 300 h in a gas mixture of 5% CO and 95% CO_2 at 1623 K. The ratio of reactants was chosen such that the composition of the final product would be slightly uranium deficient to ensure phase purity of the brannerite.

The actual composition of the uranium-containing compound was found to be $U_{0.952}Ti_{2.04806}O_6$ using XRD with a 0.31 mass% contamination of UO_2. The purity of the cerium brannerite was measured using microprobe analysis and was found to have CeO_2 as an impurity phase at a level of 0.96 mass%. No excess rutile, anatase, or other chemical impurities were found in either compound.

Calorimetric measurements

Heat capacity measurements were made on an adiabatic calorimeter of a Westrum design described previously in the literature [8–11]. In these experiments, we used a gold-plated calorimeter with a volume of 10 cm^3.

Temperatures were measured with two 25-Ω Pt resistance thermometers (SN 4335 for $CeTi_2O_6$ and SN 4253 for UTi_2O_6) manufactured by Rosemont Aerospace [12]. The thermometers were calibrated by the manufacturer over the range $13.8 \leq (T/\mathrm{K}) \leq 523$ on the ITS-90 temperature scale. The calibration was checked by measurement of the triple point of sodium sulfate decahydrate. Temperatures are believed to reproduce the ITS-90 scale to ±0.016 K for $13.8 < (T/\mathrm{K}) \leq 40$ K, and to ±0.005 K for $40 < (T/\mathrm{K}) = 523$. Calibration of the Pt thermometer (SN 4253) below T=13.8 K was performed *vs.* a germanium thermometer (SN 27277) manufactured by Lake Shore [13] and calibrated in-house *vs.* a rhodium-iron thermometer (SN B160) produced and calibrated at the National Physical Laboratory in Teddington, UK, on the ITS-90 temperature scale. Below 13.8 K, the sensitivity of this platinum thermometer is greatly reduced resulting in an estimated uncertainty in the temperature measurement of ±0.03 K.

Both samples were loaded into the adiabatic cryostat using the same procedure. A sample was placed in the calorimeter which was then evacuated on a vacuum line. A small pressure of helium gas was added to facilitate thermal conductivity and the calorimeter was sealed by pressing a gold gasket against a knife edge. Details of the loading, including sample masses, helium gas pressure, and densities used in buoyancy corrections, can be found in Table 1.

Estimates of the uncertainties of the measurements

Measurements of the standard molar heat capacity of synthetic sapphire (NIST SRM-720) were performed in separate experiments in order to assess the accuracy of the heat capacity measurements obtained from this apparatus. We compared our results to those of Archer [14] and found that our deviations are within the uncertainties quoted by Archer [14] for his values. More details about the uncertainties of the sapphire measurements have been published previously [15, 16]. The contributions of both cerium and uranium brannerite samples to the total heat capacities are much larger below 50 K than the corresponding contributions for sapphire and are tabulated in Table 1. Therefore, we estimate that the uncertainties for the measurements made on both calorimetric samples are within the stated uncertainties for synthetic sapphire.

Results

The molar heat capacities of $CeTi_2O_6$, corrected for the CeO_2 impurity (see below), are reported in Table 2, and the uncorrected molar heat capacities of 99.69mass% $U_{0.952}Ti_{2.04806}O_6$ and 0.31mass% UO_2 are given in Table 3. An additional significant figure beyond those justified based on the uncertainties are given in the tables. In Fig. 1 the molar heat capacities of cerium and uranium brannerite obtained in this study are shown in the region $20 < T/\mathrm{K} < 400$, with the results for uranium brannerite translated upwards by 10 J K^{-1} mol^{-1} for clarity. The results for $T/\mathrm{K} < 30$ are shown in the inset to Fig. 1.

Discussion

Since both compounds contained significant amounts of the respective binary oxides as impurities (UO_2 in uranium brannerite and CeO_2 in cerium brannerite), it

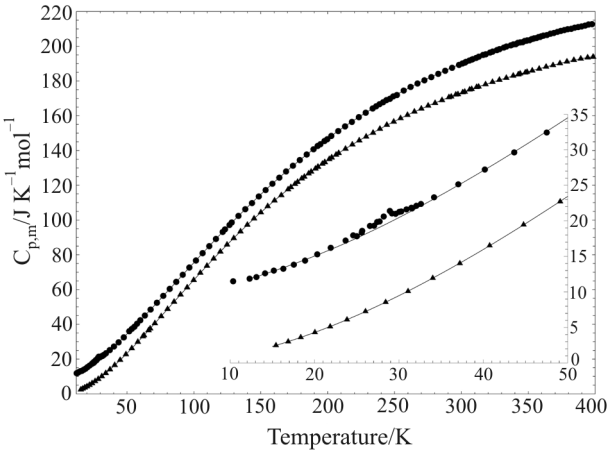

Fig. 1 Molar heat capacities of $CeTi_2O_6$ and UTi_2O_6. ▲ – $CeTi_2O_6$ experimental points; ● – UTi_2O_6 experimental points +10 J K^{-1} mol^{-1}; — – fit of the $CeTi_2O_6$ experimental results; – – – fit of the UTi_2O_6 experimental results +10 J K^{-1} mol^{-1}. The inset shows the low-temperature data on an expanded scale

Table 1 Details of the calorimetric experiments for the adiabatic measurements

10<(*T*/K)≤400 adiabatic measurements				
	$CeTi_2O_6$		UTi_2O_6	
Helium exchange gas/kPa	4.40		2.93	
Sample/g	20.8738		13.9752	
Mass% of the oxides	CeO_2	0.96	UO_2	0.31
Density/g cm^{-3}	4.952		6.39	
Contribution of sample to measured C_p at selected T	*T*/K	%	*T*/K	%
	15	57	15	44
	65	32	65	21
	250	44	250	31
	400	46	350	32
Contribution of oxides to measured C_p at selected T	*T*/K	%	*T*/K	%
	15	0.05	15	0.05
	65	0.11	65	0.03
	250	0.15	250	0.03
	400	0.16	350	0.03

was necessary to correct for the contribution of these oxides to the heat capacities. For CeO_2, a fit was made using the data from Touloukin and Buyco [17] for temperatures below 300 K. Points above T=300 K were generated from coefficients given by Robie and Hemingway [18], which they derived based on several previous measurements of the heat capacity of CeO_2.

Correcting for the presence of UO_2 in the uranium brannerite presented a more difficult problem. For temperatures above 300 K, the heat capacity of UO_2 was generated using the coefficients given by Robie and Hemingway [18]. Values for the heat capacity of UO_2 at temperatures below 300 K have been reported by several groups [19–21]. All of these measurements show a well-defined peak near 30 K, but the peak width and peak position is highly sample dependent. Since the measurements by Westrum *et al*. [19] used the highest quality UO_2 sample, we chose this data to correct for the UO_2 impurity in our uranium brannerite sample. To correct for the lattice contribution, we plotted Westrum's data [19] in the peak region and drew a smooth curve underneath the peak to represent the lattice. This lattice data was then added to the heat capacity data outside the peak region and the entire data set fit to several polynomial functions. The resulting smooth functions were used to correct for the lattice contribution of the UO_2 impurity.

The peak in the UO_2 heat capacity data near T=30 K has been attributed to a magnetic transition but, as mentioned previously, the peak width and peak position is highly sample dependent [22]. As seen in Fig. 2, the presence of the UO_2 magnetic transition is also present in the uranium brannerite data although to a significantly smaller extent. To correct for the magnetic transition, the uranium brannerite data, corrected for the UO_2 lattice, was hand plotted and a smooth line was drawn though the transition region to represent the lattice contribution. Points were taken

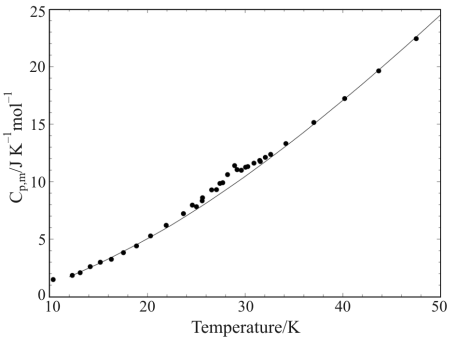

Fig. 2 Expanded view of the UO_2 impurity magnetic transition. ● – UTi_2O_6 experimental points (with UO_2 impurity). — – hand drawn extrapolated UTi_2O_6 lattice

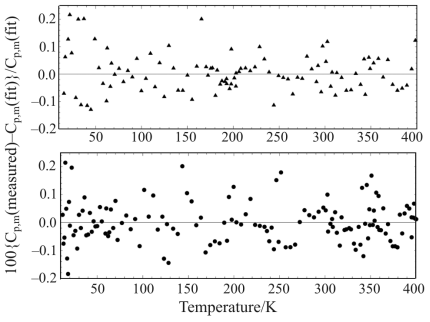

Fig. 3 Deviations of measured data from the polynomial fits. ▲ – $CeTi_2O_6$ deviations; ● – UTi_2O_6 deviations. The deviations are plotted as 100 {$C_{p,m}$(measured)–$C_{p,m}$(fit)}/$C_{p,m}$(fit)

Table 2 Experimental molar heat capacities, $C_{p,m}$, of $CeTi_2O_6$ presented in order of increasing temperature. (M=331.8464 g mol^{-1})

T/K	$C^0_{p,m}$/J K^{-1} mol^{-1}	T/K	$C^0_{p,m}$/J K^{-1} mol^{-1}	T/K	$C^0_{p,m}$/J K^{-1} mol^{-1}
15.424	2.4810	144.95	100.91	264.81	162.39
16.864	3.0103	150.03	104.40	269.97	164.07
18.356	3.6128	155.11	107.95	275.13	165.79
20.035	4.3065	160.20	111.19	280.29	167.32
21.848	5.1223	165.30	114.27	285.45	169.01
23.837	6.0938	170.40	117.66	290.62	170.65
26.030	7.2568	172.45	118.95	292.35	171.06
28.423	8.5679	175.51	120.76	295.80	172.22
31.078	10.100	177.40	121.88	297.35	172.38
34.008	11.958	180.62	123.89	300.98	173.49
37.214	14.025	182.51	124.87	302.51	173.79
40.752	16.526	185.74	126.76	306.15	175.06
44.776	19.469	187.64	127.81	307.68	175.38
49.111	22.722	190.86	129.59	311.32	176.49
53.518	26.230	192.61	130.53	312.85	176.74
58.013	29.898	192.76	130.63	318.02	178.09
61.817	33.071	195.99	132.39	323.19	179.45
62.588	33.652	197.72	133.28	328.37	180.69
66.026	36.596	197.89	133.20	333.54	181.79
67.233	37.589	201.12	135.01	338.72	183.04
70.739	40.596	202.85	135.94	342.56	183.73
75.483	44.658	203.02	135.96	343.89	184.26
80.275	48.804	206.25	137.58	347.75	184.84
85.109	52.941	208.16	138.51	349.07	185.20
89.978	57.114	213.30	141.01	352.93	185.98
94.878	61.250	218.44	143.45	358.11	187.02
99.803	65.495	223.58	145.78	363.29	188.18
104.76	69.621	228.73	147.96	368.47	189.06
109.73	73.676	233.88	150.24	373.65	190.20
114.71	77.843	239.03	152.46	378.84	191.17
119.72	81.798	244.18	154.73	384.02	192.03
124.75	85.861	249.33	156.58	389.20	192.84
129.78	89.587	254.48	158.55	394.38	193.50
134.83	93.466	259.64	160.46	398.46	193.88
139.89	97.270				

from this line from 12 to 50 K to create a smooth lattice representation through the transition region as shown in Fig. 2. This lattice data was then combined with the corrected heat capacity data outside the transition region to form the corrected uranium brannerite data set. Representative per cent contributions of both the UO_2 and CeO_2 impurities are given in Table 1.

The standard molar thermodynamic functions, $C^0_{p,m}$, $\Delta^T_0 S^0_m$, $\Delta^T_0 H^0_m$ and $\Phi=\{\Delta^T_0 S^0_m - \Delta^T_0 H^0_m/T\}$ have been generated at smoothed temperatures by fitting appropriate orthogonal polynomial functions to the impurity corrected experimental data. The results are given in Tables 4 and 5 for the cerium and uranium brannerite samples, respectively. Figure 3 shows the deviations of the fitted polynomial functions used to calculate the thermodynamic functions. As can be seen, the deviations of the fits are well within experimental uncertainties.

We have also calculated the standard molar thermodynamic functions of formation, $\Delta^T_f X^0_m$, and the

Table 3 Experimental molar heat capacities, $C^0_{p,m}$, of 99.69 mass% $U_{0.952}Ti_{2.04806}O_6$ and 0.31% UO_2 (M = 420.6524 g mol^{-1})

T/K	$C^0_{p,m}$/J K^{-1} mol^{-1}	T/K	$C^0_{p,m}$/J K^{-1} mol^{-1}	T/K	$C^0_{p,m}$/J K^{-1} mol^{-1}
10.342	1.4870	72.283	42.398	249.05	161.16
12.302	1.8476	77.053	46.352	251.68	161.88
13.106	2.0790	81.869	50.366	256.83	164.46
14.134	2.6069	86.726	54.424	261.99	166.54
15.171	2.9890	91.618	58.487	267.15	168.54
16.295	3.2460	96.541	62.677	272.32	170.37
17.533	3.8207	101.49	66.694	277.49	172.19
18.870	4.4035	106.46	70.894	282.66	174.06
20.315	5.2752	111.45	74.953	287.83	175.86
21.914	6.2001	116.46	79.122	293.00	177.56
23.677	7.2120	121.48	83.116	298.18	179.22
24.586	7.9518	123.20	84.605	300.73	180.05
25.011	7.8173	126.52	87.115	302.64	180.55
25.595	8.3318	128.22	88.559	303.35	181.01
25.634	8.5944	133.27	92.350	305.88	181.74
26.565	9.2744	138.33	96.204	307.79	182.30
27.061	9.2967	143.41	99.740	308.52	182.57
27.416	9.8392	148.49	103.54	311.04	183.23
27.705	9.9038	153.58	107.21	312.96	183.94
28.195	10.607	158.68	110.88	316.21	184.97
28.919	11.387	163.78	114.35	318.14	185.34
29.170	11.038	168.90	117.92	321.38	186.34
29.608	10.983	174.01	121.23	323.31	186.87
30.040	11.250	179.13	124.48	326.56	187.76
30.267	11.306	184.25	127.67	328.48	188.28
30.894	11.603	189.38	130.68	331.74	189.24
31.490	11.841	192.46	132.58	333.66	189.78
31.547	11.741	194.51	133.57	336.92	190.45
32.062	12.106	197.59	135.45	338.84	191.05
32.610	12.368	199.65	136.46	340.64	191.11
34.166	13.306	202.73	138.35	342.10	191.93
37.029	15.137	207.86	141.17	344.02	192.16
40.182	17.214	213.00	143.85	345.79	192.32
43.664	19.625	218.14	146.43	347.27	193.03
47.513	22.424	223.28	149.15	348.59	193.13
51.585	26.003	228.42	151.68	349.20	193.38
53.553	27.342	233.58	154.13	350.97	193.44
55.496	28.628	236.23	155.39	352.46	194.11
57.451	30.331	238.73	156.60	353.57	194.26
59.894	32.301	241.38	157.72	354.38	194.51
63.269	35.034	243.89	158.96	356.16	194.70
67.546	38.489	246.53	159.72	357.65	195.26
358.74	195.28	371.72	198.24	387.27	200.97
359.56	195.69	374.28	198.78	389.86	201.37
361.35	196.06	376.90	199.28	392.46	201.84
363.91	196.44	379.47	199.78	395.04	202.47
366.53	197.15	382.08	200.03	397.65	202.65
369.09	197.60	384.67	200.65		

Table 4. Standard thermodynamic functions of $CeTi_2O_6$. $\Phi_m^0=\Delta_0^T S_m^0-\Delta_0^T H_m^0/T$. M=331.8464 g mol^{-1} and p°=100 kPa

T/K	$C_{p,m}^0$/J K^{-1} mol^{-1}	$\Delta_0^T S_m^0$/J K^{-1} mol^{-1}	$\Delta_0^T H_m^0 T^{-1}$/J K^{-1} mol^{-1}	Φ_m^0/J K^{-1} mol^{-1}
5	0.12290	0.04175	0.03122	0.01054
10	0.85558	0.30740	0.22765	0.07975
15	2.3282	0.91125	0.66470	0.24655
20	4.2967	1.8404	1.3177	0.52268
25	6.6928	3.0488	2.1462	0.90266
30	9.4761	4.5097	3.1310	1.3787
35	12.585	6.2001	4.2559	1.9442
40	15.975	8.0989	5.5062	2.5928
45	19.611	10.188	6.8693	3.3189
50	23.445	12.451	8.3337	4.1176
60	31.527	17.434	11.520	5.9139
70	39.963	22.924	14.977	7.9463
80	48.554	28.820	18.637	10.183
90	57.127	35.035	22.438	12.597
100	65.621	41.494	26.333	15.162
110	73.955	48.141	30.285	17.856
120	82.051	54.925	34.263	20.662
130	89.845	61.803	38.241	23.562
140	97.295	68.736	42.195	26.541
150	104.38	75.692	46.107	29.585
160	111.09	82.645	49.961	32.685
170	117.44	89.572	53.745	35.827
180	123.43	96.456	57.452	39.005
190	129.08	103.28	61.075	42.208
200	134.42	110.04	64.610	45.431
210	139.45	116.72	68.055	48.667
220	144.19	123.32	71.409	51.911
230	148.66	129.83	74.671	55.158
240	152.87	136.25	77.842	58.403
250	156.83	142.57	80.924	61.643
260	160.56	148.79	83.916	64.876
270	164.06	154.92	86.820	68.097
273.15	165.11	156.83	87.717	69.110
280	167.34	160.94	89.637	71.306
290	170.42	166.87	92.370	74.499
298.15	172.78	171.63	94.536	77.090
300	173.30	172.70	95.021	77.676
310	176.01	178.42	97.590	80.834
320	178.56	184.05	100.08	83.972
330	180.97	189.58	102.50	87.088
340	183.26	195.02	104.84	90.183
350	185.44	200.36	107.11	93.255
360	187.51	205.62	109.31	96.304
370	189.45	210.78	111.45	99.328
380	191.26	215.86	113.53	102.33
390	192.88	220.85	115.55	105.30
400	194.32	225.75	117.50	108.25

Table 5 Standard thermodynamic functions of $U_{0.952}Ti_{2.04806}O_6$. $\Phi_m^0=\Delta_m^T S_m^0-\Delta_0^T H_m^0/T$. M=420.6524 g mol^{-1} and $p°$=100 kPa

T/K	$C_{p,m}^0$/J K^{-1} mol^{-1}	$\Delta_0^T S_m^0$/J K^{-1} mol^{-1}	$\Delta_0^T H_m^0 T^{-1}$/J K^{-1} mol^{-1}	Φ_m^0/J K^{-1} mol^{-1}
0	0	0	0	0
5	0.16232	0.05527	0.04130	0.01396
10	1.1071	0.40245	0.29750	0.10494
15	2.8842	1.1676	0.84744	0.32019
20	5.0491	2.2858	1.6202	0.66558
25	7.5781	3.6771	2.5526	1.1245
30	10.467	5.3090	3.6263	1.6828
35	13.650	7.1583	4.8278	2.3304
40	17.070	9.2018	6.1421	3.0597
45	20.697	11.420	7.5559	3.8639
50	24.503	13.796	9.0591	4.7370
60	32.415	18.959	12.289	6.6702
70	40.507	24.561	15.740	8.8213
80	48.845	30.512	19.355	11.157
90	57.169	36.746	23.094	13.652
100	65.566	43.204	26.922	16.283
110	73.885	49.845	30.814	19.031
120	82.008	56.624	34.744	21.880
130	89.880	63.500	38.684	24.817
140	97.485	70.441	42.614	27.828
150	104.82	77.419	46.518	30.901
160	111.87	84.410	50.383	34.027
170	118.61	91.396	54.200	37.196
180	125.04	98.359	57.958	40.401
190	131.15	105.28	61.652	43.634
200	136.94	112.16	65.272	46.888
210	142.43	118.98	68.817	50.159
220	147.62	125.72	72.282	53.441
230	152.55	132.40	75.666	56.729
240	157.20	138.99	78.967	60.019
250	161.60	145.49	82.186	63.308
260	165.74	151.91	85.320	66.593
270	169.65	158.24	88.372	69.870
273.15	170.83	160.22	89.316	70.901
280	173.32	164.48	91.341	73.138
290	176.78	170.62	94.228	76.394
298.15	179.46	175.56	96.522	79.037
300	180.06	176.67	97.035	79.636
310	183.15	182.63	99.764	82.862
320	186.07	188.49	102.42	86.072
330	188.81	194.26	104.99	89.263
340	191.36	199.93	107.50	92.435
350	193.72	205.51	109.93	95.586
360	195.90	211.00	112.28	98.716
370	197.95	216.40	114.57	101.82
380	199.88	221.70	116.79	104.91
390	201.70	226.92	118.95	107.97
400	203.33	232.04	121.04	111.01

Table 6 Thermodynamic functions of formation

Molar entropies (J K^{-1} mol^{-1})								
Ti	O_2	U	Ce	TiO_2(rutile)	UO_2	CeO_2	$CeTiO_6$	UTi_2O_6
30.759	205.147	50.2	72.0	50.6	77.0	62.3	171.63	175.56

Formation energetics						
	$\Delta_f^{298.15}S_m^0$/ J K^{-1} mol^{-1}	$\Delta_f^{298.15}H_m^0$/ kJ mol^{-1}	$\Delta_f^{298.15}G_m^0$/ kJ mol^{-1}	$\Delta_r^{298.15}S_m^0$/ J K^{-1} mol^{-1}	$\Delta_r^{298.15}H_m^0$/ kJ mol^{-1}	$\Delta_r^{298.15}G_m^0$/ kJ mol^{-1}
$CeTi_2O_6$	–557.33	–2958.4	–2786.3	8.13	18.3	15.88
UTi_2O_6	–551.60	–2809.4	–2814.7	–2.64	–6.1	–5.30

$CeTi_2O_6$	Temperature dependent thermodynamic functions			
T/K	$\Delta_f^{298.15}H_m^0$/kJ mol^{-1}	$\Delta_f^{298.15}G_m^0$/kJ mol^{-1}	$\Delta_r^{298.15H}H_m^0$/kJ mol^{-1}	$\Delta_r^{298.15}G_m^0$/kJ mol^{-1}
100	–2952.7	–2899.0	16.38	15.66
200	–2957.5	–2842.8	17.70	16.05
298.15	–2958.4	–2786.3	18.30	15.88
300	–2958.4	–2785.3	18.30	15.83
400	–2957.4	–2728.2	18.32	14.97

UTi_2O_6	Temperature dependent thermodynamic functions			
T/K	$\Delta_f^{298.15}H_m^0$/kJ mol^{-1}	$\Delta_f^{298.15}G_m^0$/kJ mol^{-1}	$\Delta_r^{298.15}H_m^0$/kJ mol^{-1}	$\Delta_r^{298.15}G_m^0$/kJ mol^{-1}
100	–2974.0	–2922.4	–6.447	–6.088
200	–2978.7	–2868.7	–6.487	–5.717
298.15	–2979.2	–2814.7	–6.100	–5.299
300	–2979.2	–2813.7	–6.089	–5.289
400	–2977.5	–2759.5	–5.593	–5.118

thermodynamic functions of formation of $CeTi_2O_6$ and UTi_2O_6 from the reaction of the binary oxides, $\Delta_r^T X_m^0$. The entropies, $\Delta_0^{298.15}S_m^0$, used to calculate $\Delta_f^{298.15}S_m^0$ and $\Delta_r^{298.15}S_m^0$ are listed in Table 6 as are the thermodynamic functions, calculated as a function of temperature. $\Delta_f^{298.15}S_m^0$ for $CeTi_2O_6$ and UTi_2O_6 are –577.33 and –551.60 J K^{-1} mol^{-1}, respectively. For the reaction of the oxides to form the brannerite compounds $\Delta_r^{298.15}S_m^0$ was found to be 8.13 and –2.64 J K^{-1} mol^{-1} for $CeTi_2O_6$ and UTi_2O_6, respectively. The Gibbs free energy of formation, $\Delta_f^{298.15}G_m^0$, was calculated using the formula $\Delta_f^T G_m^0 = \Delta_f^T H_m^0 - T\Delta_f^T S_m^0$ and was found to be –2786.3 kJ mol^{-1} for $CeTi_2O_6$ and –2814.7 kJ mol^{-1} for UTi_2O_6. Similarly, the Gibbs free energy of the reaction of the oxides forming $CeTi_2O_6$ and UTi_2O_6 were also calculated at 298.15 K using the same equation and were found to be 15.88 and –5.30 kJ mol^{-1} respectively. The temperature dependence of $\Delta_f^T H_m^0$ and $\Delta_r^T H_m^0$ was calculated [23] using the relation:

$$\Delta_r^T H_m^0 = \sum \nu_i (H_{m,T}^0 - H_{m,298}^0)_i + \Delta_r^{298.15} H_m^0$$

which then was combined with the entropy values to calculate the temperature dependence of $\Delta_f^T G_m^0$, and $\Delta_r^T G_m^0$. The values for the entropy and the thermodynamic functions of $H_{m,T}^0 - H_{m,298}^0$ for $CeTi_2O_6$ and UTi_2O_6 were obtained in this study. Entropy values and the thermodynamic functions of $H_{m,T}^0 - H_{m,298}^0$ for Ti, TiO_2 (rutile), Ce, CeO_2, U, UO_2 and O_2, were found in the JANAF Thermochemical Tables 3rd Ed. [24], in Robie and Hemingway [18], and in Pankratz [25]. $\Delta_f^{298.15}H_m^0$ and $\Delta_r^{298.15}H_m^0$ values for uranium and cerium brannerite were obtained by Putnam *et al*. [7] Additional thermodynamic values for uranium were obtained from Lang *et al*. [26].

Our results suggest that cerium brannerite is unstable with respect to the oxides and therefore a poor choice for a host matrix ceramic for nuclear materials disposal. The sign difference in the Gibb's free of the reaction with the oxides also suggests that the cerium analogue has significantly different properties than those of the uranium compound such that modeling behavior of nuclear materials using cerium compounds needs to be more closely examined.

Acknowledgements

Funding was provided by the United States Department of Energy grant number DE-FG07-97ER45673. Marcus Donaldson gratefully acknowledges financial support from the Office of Research and Creative Activities (ORCA) of Brigham Young University.

References

1 G. B. Roberts, 'Five minutes past midnight: the clear and present danger of nuclear weapons grade fissile materials', USAF Institute for National Security Studies, US Air Force Academy, 1995.
2 Management and Disposition of Excess Weapons Plutonium; National Academy of Sciences, Washington DC. 1994.
3 E. R. Merz and C. E. Walter, Eds. Disposal of Weapons Plutonium, Kluwer Academic Publishing, Dordrecht, Germany 1995.
4 W. Lutze and R. C. Ewing, Eds Radioactive Waste Forms of the Future; North-Holland Physics Publishing, Amsterdam 1988.
5 J. T. Szymanski and J. D. Scott, Can. Mineral., 20 (1982) 271.
6 A. Kahn-Harari, Revue internationale des hautes températures et des réfractaires, 8 (1971) 71.
7 R. L. Putnam, U. F. Gallegos, B. B. Ebbinghaus, A. Navrotsky, K. B. Helean, S. V. Ushakov, B. F. Woodfield, J. Boerio-Goates and M. A. Williamson, Ceram. Trans., D. R. Spearing, G. L. Smith and R. L. Putnam, Eds, 2001; Vol. 119, pp. 147–158.
8 J. Boerio-Goates and B. F. Woodfield, Can. J. Chem., 66 (1988) 645.
9 M. C. M. S. Beard, Thesis, Brigham Young University, 1998.
10 E. H. Battley, R. L. Putnam and J. Boerio-Goates, Thermochim. Acta, 298 (1997) 37.
11 B. F. Woodfield, J. L. Shapiro, R. Stevens and J. Boerio-Goates, J. Chem. Thermodyn., 31 (1999) 1573.
12 Rosemont Aerospace, 12256 Trapp Road, Eagan, MN, 55121, USA.
13 Lake Shore Cryotronics, Inc., 575 McCorkle Blvd., Westerville OH, 43082, USA.
14 D. G. Archer, J. Phys. Chem. Ref. Data, 22 (1993) 1441.
15 J. Boerio-Goates, R. Stevens, B. K. Hom, B. F. Woodfield, P. M. Piccione, M. E. Davis and A. Navrotsky, J. Chem. Thermodyn., 34 (2002) 205.
16 J. Boerio-Goates, M. R. Francis, R. N. Goldberg, M. A. V. Ribeiro da Silva, M. D. M. C. Ribeiro da Silva and Y. B. J. Tewari, Chem. Thermodyn., 33 (2001) 929.
17 Y. S. Touloukian and E. H. Buyco, In Thermophysical Properties of Matter, 5 (1970) 63.
18 R. A. Robie and B. S. Hemingway, 'Thermodynamic Properties of Minerals and Related Substances at 298.15 K and 1 Bar (10^5 Pascals) Pressure and at Higher Temperatures', U. S. Geological Survey Bulletin, 1995.
19 E. F. Westrum Jr. and J. J. Huntzicker, J. Chem. Thermodyn., 3 (1971) 61.
20 Y. S. Touloukian and E. H. Buyco, In Thermophysical Properties of Matter, 1970; Vol. 5, p. 260.
21 W. M. Jones, J. Gordon and E. A. Long, J. Chem. Phys., 20 (1952) 695.
22 J. J. Huntzicker and E. F. Westrum Jr., J. Chem. Thermodyn., 3 (1971) 61.
23 J. B. Ott and J. Boerio-Goates, 'Chemical Thermodynamics: Principles and Applications', Academic Press, London 2000.
24 M. W. Chase Jr., C. A. Davies, J. R. Downey Jr., D. J. Frurip, R. A. McDonald and A. N. Syverud, J. Phys. Chem. Ref. Data, 14 (1985) suppl. 1.
25 L. B. Pankratz, 'Thermodynamic Properties of Elements and Oxides' United States Department of the Interior, Washington DC. 1982.
26 B. E. Lang, M. H. Donaldson, B. F. Woodfield, J. Boerio-Goates and J. C. Lashley, J. Chem. Thermodyn., submitted

DOI: 10.1007/s10973-005-7091-z